Optical Spectra of Lactoperoxidase as a Function of Solvent†

B. Zelent,‡ T. Yano,‡ P.-I. Ohlsson,§ M. L. Smith,|| J. Paul,⊥ and J. M. Vanderkooi*,‡

Johnson Research Foundation, Department of Biochemistry and Biophysics, School of Medicine, University of Pennsylvania, Philadelphia, Pennsylvania 19104, Department of Plant Physiology, Umeå Universitet, S0910 87 Umeå, Sweden, Anabolic Laboratories, Tempe, Arizona 85281, and Division of Physics, Luleå University of Technology, 971 87 Luleå, Sweden

Received July 14, 2005; Revised Manuscript Received September 16, 2005

ABSTRACT: The iron of lactoperoxidase is predominantly high-spin at ambient temperature. Optical spectra of lactoperoxidase indicate that the iron changes from high-spin to low-spin in the temperature range from room temperature to 20 K. The transformation is independent of whether the enzyme is in glycerol/water or solid sugar glass. Addition of the inhibitor benzohydroxamic acid increases the amount of the low-spin form, and again the transformation is independent of whether the protein is in an aqueous solution or a nearly anhydrous sugar. In contrast to lactoperoxidase, horseradish peroxidase remains high-spin over the temperature excursion in both solvents and with addition of benzohydroxamic acid. We conclude that details of the heme pocket of lactoperoxidase allow ligation changes with temperature that are dependent upon the apoprotein but independent of solvent fluctuations. At low pH, lactoperoxidase shows a solvent-dependent transition; the high-spin form is predominant in anhydrous sugar glass, but in the presence of water, the low-spin form is also present in abundance. The active site of lactoperoxidase is not as tightly constrained at low pH as at neutrality, though the enzyme is active over a wide pH range.

Lactoperoxidase (LPO)[1] is a heme enzyme that was originally found in milk (*1*). It is now identified in other exocrine secretions, including sweat, saliva, cervical fluid, tears, and lung surfactant (*2*, *3*). LPO catalyzes the oxidation of SCN^- by H_2O_2 to form $OSCN^-$; this product is a highly reactive oxidizing agent that destroys bacteria, fungi, and viruses. In so doing, LPO acts in the first line of defense against pathogens (*4*, *5*). This activity prevents many pathogens from entering the mammalian body where they signal the synthesis of a sister enzyme, myeloperoxidase (MPO). LPO and other mammalian peroxidases have the ability to bind many small anions either directly to heme iron or within a few angstroms of the porphyrin, depending upon the particular anion (*6*). One toxic byproduct of MPO from bromide ion and peroxide is OBr^-, a well-known mutagen; LPO does not catalyze this reaction (*7*).

As an extracellular protein, LPO must be active at various solvent pH's, viscosities, and salinities, which implies that LPO is a stable enzyme under many conditions. In fact, LPO exhibits excellent in vitro stability under many conditions (*8*, *9*). LPO is a rather large heme enzyme with eight disulfide linkages, and the heme is covalently attached to the polypeptide by ester linkages through the 1-methyl- and 5-methylporphyrin substituents (*10*). These linkages have also been observed for MPO, where the heme is also attached to the polypeptide through an unusual sulfonium linkage (*11*, *12*), which has been postulated to also act inductively, removing electron density from the iron toward the porphyrin periphery. These interesting and unusual bonds keep the heme firmly attached to the protein, not allowing dissociation under even harsh conditions. In contrast, protoheme is readily dissociated from plant peroxidases into aqueous buffers under mild conditions (*13*). The bonds between the heme and polypeptide might also be in part responsible for the higher Fe(III)/Fe(II) reduction potential of mammalian peroxidases in contrast to those of plant peroxidases (*14*). Both these results and the crystallographic structure of MPO suggest a large arena for enzymatic activity, distal to LPO heme, not only apparently open to water but also well-controlled by the protein (*11*). How nearby water affects the electrochemical potential and selectivity of heme protein activities has been a fundamental question in this field for decades (*15*).

Whether protein dynamical modes are coupled to solvent modes is relevant to enzyme function. Heme proteins have proven to be especially useful in addressing this question. Austin et al., using infrared spectroscopy, demonstrated the presence of dynamically interconverting conformational substates in myoglobin (*16*). Computations of heme optical spectra give a firm basis for the correlation of protein conformations with spectral bandwidths (*17*−*20*). In view of the wide range of functions of heme proteins, from a carrier of small molecules to electron transfer and redox reactions, it stands to reason that dynamical correlations among the solvent, polypeptide chain, and prosthetic group vary considerably among different heme proteins. This premise can be examined by comparing different heme proteins. To distinguish between solvent-slaved and solvent-independent motions, various solvents and a wide range of temperatures should be used. With decreasing temperatures,

† This work was supported by National Institutes of Health Grant GM P01 48130.

* To whom correspondence should be addressed. Telephone: (215) 898-8783. E-mail: vanderko@mail.med.upenn.edu.

‡ University of Pennsylvania.

§ Umeå Universitet.

|| Anabolic Laboratories.

⊥ Luleå University of Technology.

[1] Abbreviations: LPO, lactoperoxidase; HRP, horseradish peroxidase; BHA, benzohydroxamic acid.

10.1021/bi0513655 CCC: $30.25
Published on Web 11/08/2005

the thermal energy and mobility of all groups are reduced. When the heme is isolated from the solvent by the polypeptide chain, the heme's spectral temperature dependence will not follow the temperature dependence of the solvent. By this means, solvent-dependent and -independent effects can be separated.

In this paper, heme visible absorption spectra, as functions of solvent and temperature, are used to characterize lactoperoxidase (LPO). Resting LPO displays a high-spin ferric form with an absorption band at >600 nm. This band is polarized in the *z* direction, and it is attributed to a charge transfer transition from the a_{2u} HOMO of the porphyrin to the d_{xy}/d_{yz} orbital of the metal (*21*, *22*). In this paper, we report that ferric LPO undergoes a spin state change from high-spin to low-spin with a decrease in temperature, but without the common appearance of fine structure. Under most conditions, this change is independent of the solvent, i.e., whether the protein is in a glycerol/water mixture or in a nearly water-free sugar glass. At low pH, however, the spin state change becomes a function of solvent. In contrast, horseradish peroxidase (HRP) remains high-spin over the temperature range of 300−20 K, although the spectral resolution increases as the temperature decreases and the resolution is dependent upon solvent (*23*). The results are discussed in terms of subtle temperature-dependent changes within the LPO heme pocket, including the lack of water solvation about the heme of LPO in contrast to that of HRP.

MATERIALS AND METHODS

Materials. Water was deionized and then glass distilled. LPO from unpasteurized bovine milk was isolated by using the method of Paul et al. (*2*). Glycerol (99%), α-D-glucopyranosyl α-D-glucopyranoside [D-(+)-α-trehalose], α-D-glucopyranosyl β-D-fructofuranoside (sucrose), and, for some experiments, LPO were supplied by Sigma Chemical Co. (St. Louis, MO). LPO from Sigma, with a Reinheitzahl (RZ) value (A_{412}/A_{280}) equal to ∼1, was used without further purification. The concentrations of LPO was calculated using an extinction coefficient ϵ_{412} of 112 cm^{-1} mM^{-1} (*24*).

Sugar Glass Preparation. LPO was incorporated into trehalose/sucrose (TS) glass as described previously for other proteins (*25*). Trehalose (300 mg) and sucrose (300 mg) were dissolved in 500 μL of distilled water to form the TS stock solution. Samples were prepared as 450 μL solutions containing 150 μL of a 250 μM LPO solution, 200 μL of 10 mM potassium phosphate buffer, and 100 μL of the TS stock solution. The pH of the sample was adjusted to 3, 7, or 9. Following this step, the sample was placed on a 25 mm quartz plate 2 mm in thickness (Escoproducts, Oak Ridge, NJ) and allowed to solidify as water evaporated on a VWR Scientific Products Heat Block at 65 °C for 2 h. The resulting sugar glasses were hard to the touch and optically clear. LPO has been shown to be stable in aqueous solution to 70 °C (*9*). To achieve hydrated glasses (used in Figure 9), the glass was equilibrated in the room (30% relative humidity) or above saturated ammonium nitrate; this gives 65% relative humidity. The time of equilibration was ∼15 h at 20 °C. When the sugar glass is equilibrated at 65% relative humidity, the water/sugar molar ratio is ∼2, as determined by infrared analysis (*25*).

Cryosolution Preparation. LPO in a glycerol/aqueous buffer system was prepared by first preparing the protein in 10 mM potassium phosphate buffer. Glycerol was then added to the solution to obtain a 60% (w/w) glycerol/aqueous buffer. The pH of the sample was adjusted to 3, 7, or 9.

UV−Visible Absorption Spectroscopy. Visible absorption spectra were measured using a Hitachi Perkin-Elmer (Newtown, PA) U-3000 spectrophotometer. Samples were placed between circular quartz plates separated with a 200 μm Teflon spacer. The sample temperature for temperature-dependent absorption measurements was regulated using an APD closed cycle Helitran cryostat (Advanced Research Systems, Allentown, PA). A chamber was constructed to alleviate strain on windows due to contraction at low temperatures. For visible absorption measurements, the outer windows of the compartment were made of quartz and the inner windows were made of sapphire. The temperature was measured and controlled using a silicon diode near the sample connected to a model 9650 temperature controller (Scientific Instruments, Palm Beach, FL). Temperature-dependent measurements were performed from high to low temperatures at 10 K increments. Most spectra were taken at 1 nm spectral resolution, but some spectra were observed at 0.5 and 0.1 nm spectral resolution, to search for fine structure.

RESULTS

Optical Spectra of LPO in Sugar Glasses and Glycerol/Water Mixtures. Clear matrices that are suitable for optical studies of proteins were prepared using two cryosolvents commonly used to study proteins: glycerol/water and sugar glasses (*25*−*27*).

The spectrum for Fe(III)-bound LPO in sugar glass made of trehalose and sucrose is shown in Figure 1A. The Soret peak is at 412 nm, and the visible spectrum exhibits maxima at 500, 542, 585, and 630 nm. These values are the same as what was previously reported for LPO in aqueous buffer (*28*). The band at 630 nm is characteristic of a charge transfer band (*21*, *22*) and demonstrates that the ferric ion of LPO is high-spin at room temperature. However, at 14 K the iron becomes low-spin, which is shown by diminution of the charge transfer absorbance at 630 nm, and the shift of the Soret peak maximum to a higher wavelength and absorbance. The absorbance maxima are presented in Table 1.

The temperature dependence of the spin state transformation of LPO exhibits continuous change in spectra with the temperature decline, as is documented for the visible range in Figure 1B where spectra taken over the entire, wide temperature range are shown.

The spectra given in Figure 1B point to the existence of isosbestic points; isosbestic points would definitely prove the existence of only two species. But an expanded picture (Figure 2) shows that the crossover point is close but not rigorously exact. As the temperature decreases, the optical spectral bands of heme proteins in general become sharper (*23*, *29*). The data are therefore consistent with two temperature-dependent processes: the major factor is the shift from high-spin to low-spin, while spectral band sharpening as the temperature decreases is more subtle.

Figure 3 shows the absorbance at the peak values of 500, 542, 580, and 630 nm over the entire temperature excursion. When absorbance at one wavelength decreases, absorbance at another wavelength increases, consistent with a two-state model and equilibrium between low- and high-spin forms.

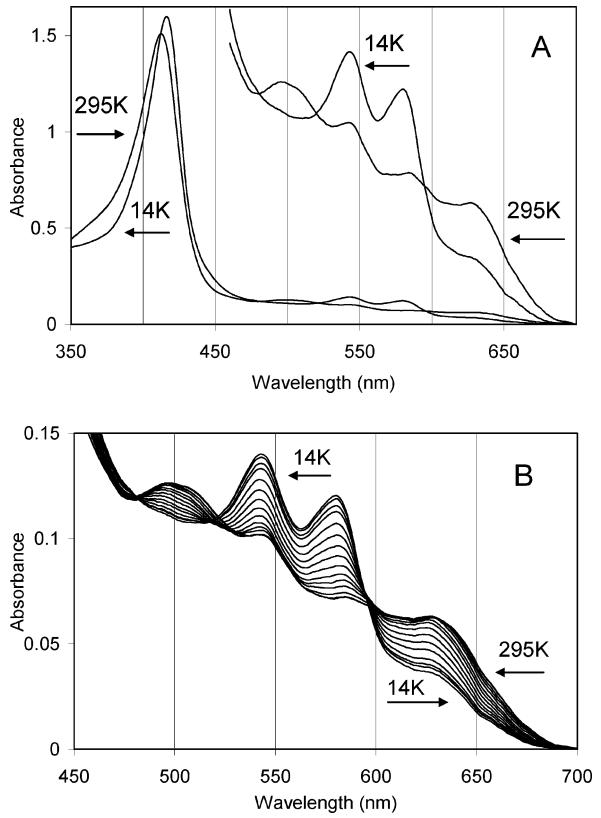

FIGURE 1: (A) UV−visible absorption spectra of LPO. LPO in TS glass at pH 7 measured at 295 and 14 K. Sample prepared as described in Materials and Methods. (B) Visible absorption bands of LPO. LPO in TS glass at pH 7 over a range of temperatures. The temperature was varied from 290 to 20 K in 20 K increments.

Table 1: Optical Properties of Fe(III)-Bound LPO[a]

complex	Soret band (nm)	visible bands (nm)	temp (K)
LPO in phosphate (pH 7)	412	500, 542, 585, 630	295
LPO in TS (pH 7)	412	500, 542, 585, 630	295
	416	−, 543, 580, 630	14
LPO in TS (pH 9)	412	500, 543, 586, 630	295
	416	−, 543, 580, 630	14
LPO in glycerol/water (pH 7)	412	500, 544, 586, 631	295
	417	−, 543, 581	120
	417	−, 543, 580	12
LPO in glycerol/water (pH 9)	412	500, 545, 586, 631	295
	414	−, 542, 580, 626	120
LPO and BHA in TS (pH 7)	417	−, 545, 580, 632w	295
	419	544, 577	12
LPO and BHA in glycerol/water (pH 7)	416	545, 582, 631m	295
	420	544, 577	120
LPO in TS (pH 3)	413	505, 545, 588, 630	295
	414	500, 542, 580, 630	14
LPO in glycerol/water (pH 3)	414	500, 544, 588, 631	295
	418	−, 542, 578	130

[a] TS refers to trehalose/sucrose glass, and glycerol/water is a 60/40 (w/w) solution. Details of sample preparation are found in Materials and Methods. W means weak and m medium.

Temperature-dependent spin state change was also seen for LPO in glycerol/water systems. The spectra at high, intermediate, and low temperatures are given in Figure 4. Spectra of Fe(III)-bound LPO at 20 °C in aqueous phosphate buffer (not shown), the glycerol/water system (Figure 4), and sugar glass composed of trehalose and sucrose (Figure 1) all match within experimental resolution.

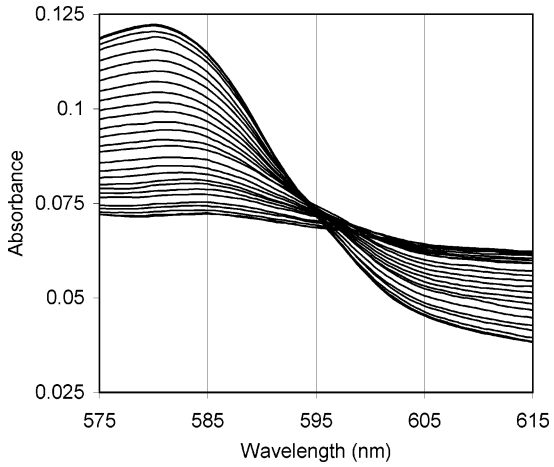

FIGURE 2: Spectra from Figure 1B are replotted, showing the gradual movement of the isosbestic point as a function of temperature.

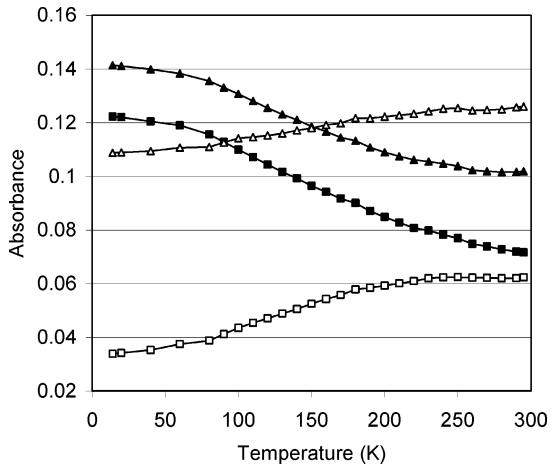

FIGURE 3: Temperature-dependent absorption maxima of visible absorption bands. LPO in TS glass at pH 7. Closed square: 580 nm; open square: 630 nm; closed triangle: 542 nm; open triangle: 500 nm.

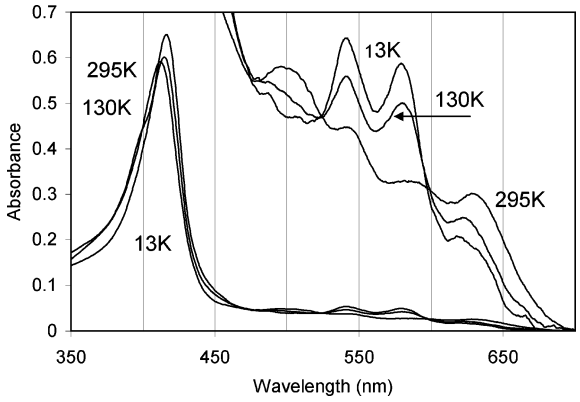

FIGURE 4: UV−visible absorption spectra of LPO in a glycerol/water mixture (60/40, v/v) at pH 7.

The changes in spectra of LPO in either solid sugar glass or in the glycerol/water system are reversible when the sample previously held at low temperatures was returned to intermediate and high temperatures, i.e., room temperature. In another experiment, LPO in the glycerol/water system was held at 150 K for 240 min; during this time, no change in the spectrum was detected. The spectra were also compared at 0.5 and 0.1 nm spectral resolution. Examination of the

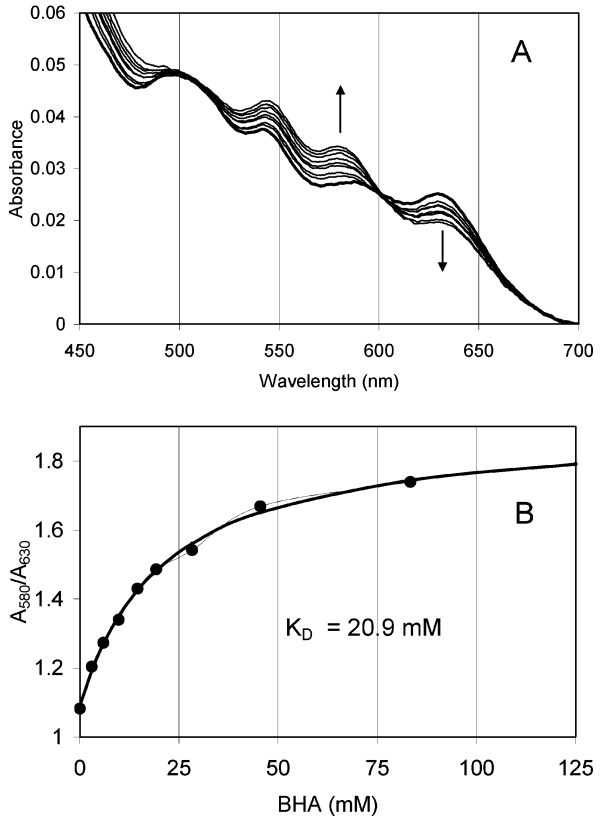

FIGURE 5: (A) Effect of BHA on the absorption spectra of 5.3 μM LPO in a glycerol/water mixture at pH 7. The thick line shows no addition. Arrows indicate the spectra in increasing amounts of BHA. Concentrations in millimolar are given in the inset. (B) Ratio of absorption bands at 580 nm to 630 nm for LPO in a glycerol/water mixture (50/50, v/v) with BHA concentration. Data were fit to the saturation function $Y = Y_0 + (Y_{Sat} - Y_0)[[BHA]/([BHA] + K_D)]$; the calculated dissociation constant $K_D = 20.9$ mM.

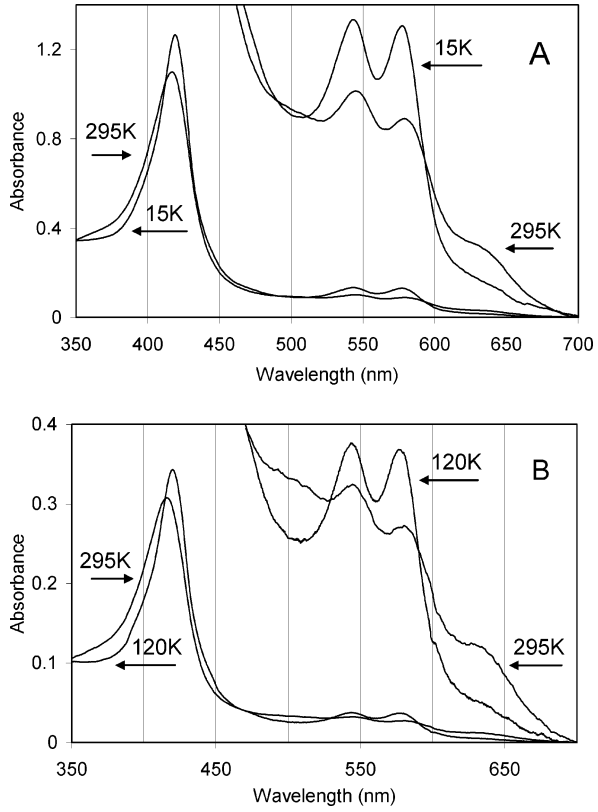

FIGURE 6: (A) UV−visible absorption spectra of LPO with BHA. LPO and 50 mM BHA were prepared in sugar glass at pH 7. Spectra measured at 295 and 15 K. (B) UV−visible absorption spectra of LPO with BHA. LPO and 50 mM BHA in a glycerol/water mixture (60/40, v/v) at pH 7. Spectra measured at 295 and 120 K.

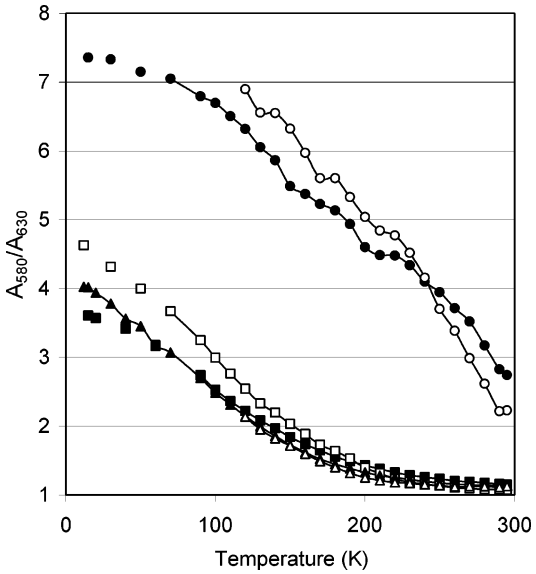

FIGURE 7: Temperature dependence of absorption bands. Ratio of absorption at 580 nm to 630 nm for LPO in sugar glass (filled symbols) and a glycerol/water mixture (empty symbols). Squares are data for LPO at pH 7, triangles for LPO at pH 9, and circles for LPO at pH 7.0 with BHA. The BHA concentration was 50 mM.

spectra under resolved conditions was of interest because the spectrum of horseradish peroxidase (HRP) exhibits vibrational fine structure at low temperatures (*21*−*23*). For LPO, there was no detectable change with an increase in spectral resolution; unlike HRP, vibronic resolution was not observed for any LPO experiment.

Addition of Inhibitor to LPO. Several studies indicate that the heme site in LPO is accessible to small inorganic substrates, whereas more bulky organic substrates do not appear to bind within the heme pocket (*14*, *30*). Benzohydroxamic acid (BHA) is a strong competitive inhibitor of HRP (*31*), with the binding having a large effect on the optical properties of the heme and heme derivatives (*32*, *33*). Addition of BHA to ferric LPO in the glycerol/water system causes a small shift in the heme absorption spectrum (Figure 5A), and the titration yields a normal binding curve with a K_d of 20.9 mM (Figure 5B). The calculated binding constant was ~3 orders of magnitude lower than that reported for binding of BHA to HRP (*34*).

BHA remains bound at low temperatures, as can be surmised from peak positions of spectra of LPO recorded at low temperatures in sugar glass (Figure 6A) and the glycerol/water system (Figure 6B). The peak positions at ~ 120 K are at 420, 544, and 577 nm, which compare with values of 417, 543, and 581 nm, respectively, for the noncomplexed form (Table 1). It was also noted that the iron remains ferric when BHA is added to resting Fe(III)-bound LPO. As reported (*35*), the Fe(II)−LPO spectrum is quite distinct from the spectra shown above.

Spin State Change as a Function of Temperature. The data presented above are summarized in Figure 7, which displays the ratio of the 580 nm/630 nm absorbance maxima as a function of temperature. Note that the profiles were only mildly influenced by the matrix, as can be seen by comparing

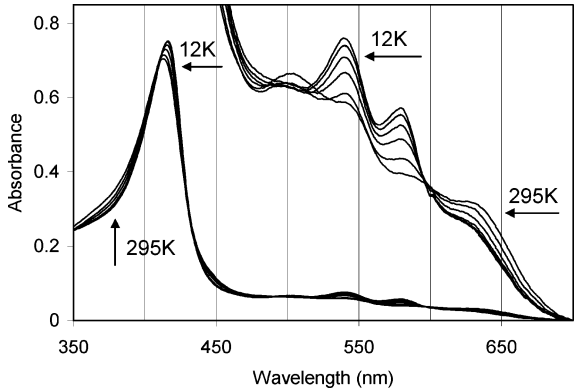

FIGURE 8: UV−visible absorption spectra of LPO. LPO in sugar glass at pH 3 measured at 295 and 12 K (indicated). Other temperatures were 100, 150, 200, and 250 K. The sample was equilibrated at 65% relative humidity and 20 °C overnight as described in Materials and Methods.

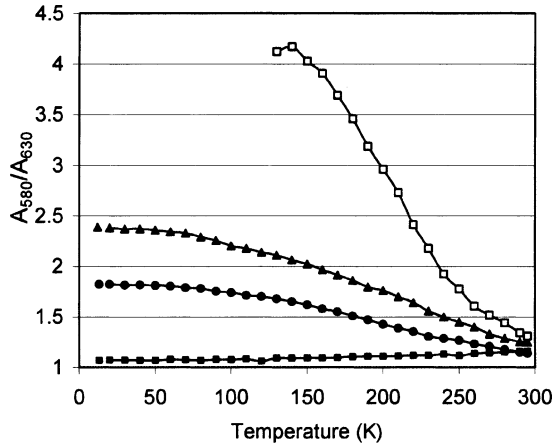

FIGURE 9: Temperature dependence of absorption bands for LPO at pH 3. Filled symbols are for sugar glass: (■) anhydrous sugar glass, (●) sugar glass equilibrated at ~30% humidity, (▲) sugar glass at 65% humidity. The empty squares are for the glycerol/water mixture (60/40, v/v).

filled symbols (sugar glass) and empty symbols (glycerol/water). A second point is that binding of BHA drastically increases the temperature of conversion from high-spin to low-spin. This effect is very dramatic; the temperature profiles reflect a ~200 K shift in temperature for the high- to low-spin transition, relative to that of the free enzyme.

Spin State Change for LPO at Low pH. It appears that the protein, not the solvent, determines the spin state changes of LPO. A question is whether this is true for LPO under all conditions. Lowering the pH results in a less well-defined protein for many heme proteins (*36*), but it has been reported that LPO is very stable under extreme conditions (*9*). For LPO, the spectrum at pH 3.0 is given in Figure 8. At room temperature, the spectrum for LPO is the same for sugar glass and glycerol/water matrices. However, for LPO at pH 3, there are interesting differences in the two matrices with a decrease in temperature. In the glycerol/water matrix, the transition of LPO to low-spin occurs with an inflection at around 200 K (Figure 9), ~100 K higher than observed at pH 7 (see Figure 7). For LPO in dry sugar or glass, the sample remains high-spin over the entire temperature decline, as seen by the filled squares in Figure 9. When the glass sample is partially hydrated, some of the sample is then converted to the low-spin form as the temperature decreases, and this conversion to low-spin is dependent on water hydration (circles and triangles).

DISCUSSION

Resting Fe(III)-bound LPO at room temperature is high-spin as presented in panels A and B of Figure 1, consistent with optical spectra (*35*, *37*) and NMR measurements (*38*, *39*). The spin state of LPO is very sensitive to temperature, and it was of interest to see whether the spin state is influenced by the medium. To test this, we examined spectra of LPO in two solvents. We have previously shown by the IR absorption of amide I band that proteins are stable in sugar glass over a temperature excursion of 10−300 K (*27*). The IR amide I bands of surface amide groups of HRP (*40*) and model peptides (*41*) in glycerol/water solutions show spectral shifts consistent with an increased level of H-bonding of exposed groups to the solvent as the temperature decreases, but the structure is maintained at low temperatures. Bulk water can also rearrange in cryogenic solvents, as indicated by IR spectral shifts occurring at even low temperatures (*42*). Water inside the heme pocket of heme proteins may well rearrange with temperature changes.

The procedures for making the matrices are quite different and should influence the protein solvation. Sugar glass, prepared at 65 °C, remains a solid over the temperature excursion here. In contrast, the glycerol/water matrix is liquid at ambient temperature and undergoes a glass transition at ~140 K, as indicated by infrared spectroscopy (*42*). The solvent, whether sugar glass or glycerol/water matrix, has an influence on inhomogeneous broadening of optical lines for other heme proteins. The effect of solvent on inhomogeneous broadening for low-spin ferrous cytochrome *c* was quantified by comparison of optical and molecular dynamics (*20*). The conclusion was that internal dynamics has a stronger effect on the inhomogeneous broadening than solvent-dependent motions, but the broadening due to the solvent was larger in sugar glass than in the glycerol/water matrix. For heme proteins that carry oxygen, broadening of the Soret band is also attributed to dynamical modes of the solvent (*17*, *43*). The activity of bulk water with the exposed porphyrin periphery is paramount for oxygen-carrying heme proteins (*15*, *44*).

We observed the spin state change of LPO usually occurred over a small temperature range, irrespective of whether the protein was in a glycerol/water matrix or sugar glass. Our results are consistent with a loosely bound water (to iron) present in the high-spin LPO at room temperature, independent of solvent. As the temperature is lowered, the low-frequency vibrational modes of water are no longer excited and water is drawn more closely to iron, giving the spectrum a more low-spin appearance. In contrast, the presence of BHA shifts the temperature dependence of the spin state toward a much higher value (Figure 7), a shift of ~200 °C. It appears that BHA binds preferentially to the low-spin form of LPO, thereby stabilizing it. Myeloperoxidase is also reported to exhibit a temperature dependence of the spin state (*45*). The two mammalian enzymes, MPO and LPO, act in contrast to the plant peroxidase, HRP. HRP, either without BHA or with BHA, and irrespective of solvent, remains high-spin over this temperature range (*46*).

Since spin state change occurs with a change in the doming of the heme, and certainly with a change in iron-ligand

interaction, the spin state change implies a rather large change in the position of atoms in LPO as a function of temperature. Low-spin heme proteins are always hexacoordinated and usually by two nitrogenous *z*-axial ligands (*47*). We should consider the possibility that the nitrogen of BHA directly ligates to iron, which was suggested for MPO, where BHA binding also yields the low-spin state (*46*). The temperature dependence of the LPO spin state shift suggests there is a ligand near the iron that, with a decrease in the level of thermal motion, is able to ligate iron. This ligation is seen both in the "liquid" (glycerol/water) and in the "solid" (sugar glass) matrices. His-226, which is a catalytic residue, and Arg-372 potentially provide electron donation on the distal side of the heme pocket (*48*). To accomplish a reorientation of porphyrin and iron, the distal ligand, probably His-226, must change geometry with BHA binding, concomitantly releasing the iron-bound water of the high-spin heme.

At low pH, the temperature dependence of LPO becomes very sensitive to the matrix effects (though LPO retains activity even at this low pH). In nearly anhydrous sugar, LPO remains high-spin. When the sugar glass is allowed to incorporate some water, there is a transition to the low-spin form, and the amount of the low-spin form increases with an increase in the amount of water (Figure 9). LPO now acts like myoglobin, where there is a mixture of spin states (*49*) and the temperature dependence is water-dependent (*50*). Since water, with its large dipole moment, effectively shields charges, the change in water position itself may be enough to influence spin. The presence of water in the heme pocket is, for example, suggested to determine the redox behavior of the iron (*15*), and water can also directly polarize the electrons in the porphyrin structure (*51*). Furthermore, the ability of water to rearrange may help to prevent the surrounding protein residues from being trapped in shallow potential wells; in this sense, water acts as a plasticizer. Eventually, however, a temperature is reached where the protein conformations are trapped in perhaps a few low-energy conformations, and there is no further change in the spin state. The data of Figure 9 are particularly interesting, since the amount of low-spin iron formed depends on the presence of water. Once the low temperature is reached, the distribution between proteins in the high- and low-spin states becomes static, and there is a mixture of the two spin forms.

To summarize, LPO at neutrality undergoes a spin state change with temperature that is solvent-independent. At low pH, the LPO active site becomes more open to solvent effects despite the rigid framework of the surrounding protein. Addition of the classic peroxidase inhibitor, benzohydroxamic acid, encourages the low-spin state and probably iron ligation by distal His-226. In contrast, HRP remains in the high-spin state at all temperatures, and the resolution of the optical spectra is dependent upon water. Relative to HRP, the active sites of LPO and MPO are more controlled by protein constraints and less by solvent interactions.

ACKNOWLEDGMENT

We thank the many conversations and encouragements of Professors Karl-Gustav Paul and Britton Chance.

REFERENCES

1. Tenouvo, J. O. (1985) in *Lactoperoxidase System: Chemistry and Biological Significance* (Pruitt, K. M., and Tenovuo, J., Eds.) pp 101−122, Dekker, New York.
2. Paul, K. G., Ohlsson, P. I., and Henriksson, A. (1980) The isolation and some liganding properties of lactoperoxidase, *FEBS Lett. 110*, 200−204.
3. Kussendrager, K. D., and van Hooijdonk, A. C. (2000) Lactoperoxidase: Physico-chemical properties, occurrence, mechanism of action and applications, *Br. J. Nutr. 84* (Suppl. 1), S19−S25.
4. Ratner, A. J., and Prince, A. (1999) Lactoperoxidase. New recognition of an "old" enzyme in airway defenses, *Am. J. Respir. Cell Mol. Biol. 20*, 642−644.
5. Wijkstrom-Frei, C., El-Chemaly, S., Ali-Rachedi, R., Gerson, C., Cobas, M. A., Forteza, R., Salathe, M., and Conner, G. E. (2003) Lactoperoxidase and human airway host defense, *Am. J. Respir. Cell Mol. Biol. 29*, 206−212.
6. Ferrari, R. P., Ghibaudi, E. M., Traversa, S., Laurenti, E., Gerson, C., Cobas, M. A., Forteza, R., Salathe, M., and Conner, G. E. (2003) Spectroscopic and binding studies on the interaction of inorganic anions with lactoperoxidase, *J. Inorg. Biochem. 68*, 17−26.
7. Henderson, J. P., Byun, J., Williams, M. V., Mueller, D. M., McCormick, M. L., and Heinecke, J. W. (2001) Production of borminating intermediates by myeloperoxidase, *J. Biol. Chem. 276*, 7867−7875.
8. Mansson-Rahemtulla, B., Rahemtulla, F., Baldone, D. C., Pruitt, K. M., and Hjerpe, A. (1988) Purification and characterization of human salivary peroxidase, *Biochemistry 27*, 233−239.
9. Paul, K. G., and Ohlsson, P. I. (1985) in *The Lactoperoxidase System: Chemistry and Biological Significance* (Pruitt, K. M., and Tenouvo, J. O., Eds.) pp 15−29, Dekker, New York.
10. Rae, T. D., and Goff, H. M. (1998) The heme prosthetic group of lactoperoxidase. Structural characteristics of heme 1 and heme 1-peptides, *J. Biol. Chem. 273*, 27968−27977.
11. Fiedler, T. J., Davey, C. A., and Fenna, R. E. (2000) X-ray crystal structure and characterization of halide-binding sites of human myeloperoxidase at 1.8 Å resolution, *J. Biol. Chem. 275*, 11964−11971.
12. Kooter, I. M., Moguilevsky, N., Bollen, A., van der Veen, L. A., Otto, C., Dekker, H. L., and Wever, R. (1999) The sulfonium ion linkage in myeloperoxidase, *J. Biol. Chem. 274*, 26794−26802.
13. Smith, M. L., Paul, J., Ohlsson, P.-I., Hjortsberg, K., and Paul, K. G. (1991) Heme-protein fission under nondenaturing conditions, *Proc. Natl. Acad. Sci. U.S.A. 88*, 882−886.
14. Ohlsson, P. I., and Paul, K. G. (1983) The reduction potential of lactoperoxidase, *Acta Chem. Scand. B37*, 917−921.
15. Stellwagen, E. (1978) Haem exposure as the determinate of oxidation−reduction potential of haem proteins, *Nature 275*, 73−74.
16. Austin, R. H., Beeson, K. W., Eisenstein, L., Frauenfelder, H., and Gunsalus, I. C. (1975) Dynamics of ligand binding to myoglobin, *Biochemistry 14*, 5355−5373.
17. Cordone, L., Cottone, G., Giuffrida, S., Palazzo, G., Venlturoli, G., and Viappiani, C. (2005) Internal dynamics and protein-matrix coupling in trehalose coated proteins, *Biochim. Biophys. Acta 1749* (2), 252−281.
18. Leone, M., Cupane, A., Vitrano, E., and Cordone, L. (1992) Strong vibronic coupling in heme proteins, *Biophys. Chem. 42*, 111−115.
19. Kaposi, A. D., Prabhu, N. V., Dalosto, S. D., Sharp, K. A., Wright, W. W., Stavrov, S. S., and Vanderkooi, J. M. (2003) Solvent dependent and independent motions of CO-horseradish peroxidase examined by infrared spectroscopy and molecular dynamics calculations, *Biophys. Chem. 106*, 1−14.
20. Prabhu, N. V., Dalosto, S. D., Sharp, K. A., Wright, W. W., and Vanderkooi, J. M. (2002) Optical spectra of Fe(II) cytochrome *c* interpreted using molecular dynamics simulations and quantum mechanical calculations, *J. Phys. Chem. B 106*, 5561−5571.
21. Eaton, W. E., and Hochstrasser, R. M. (1967) Electronic spectrum of single crystals of ferricytochrome-*c*, *J. Chem. Phys. 46*, 2533−2539.
22. Makinen, M. W., and Churg, A. K. (1983) in *Iron Porphyrins* (Lever, A. B. P., and Gray, H. B., Eds.) pp 141−235, Addison-Wesley, Reading, MA.
23. Zelent, B., Kaposi, A. D., Nucci, N. V., Sharp, K. A., Dalosto, S. D., Wright, W. W., and Vanderkooi, J. M. (2004) Water channel of horseradish peroxidase studied by the charge-transfer absorption band of ferric heme, *J. Phys. Chem. B 108*, 10317−10324.
24. Carlstrom, A. (1969) Lactoperoxidase. Some spectral properties of a haemoprotein with a prosthetic groups of unknown structure, *Acta Chem. Scand. B23*, 203−212.

25. Wright, W. W., Guffanti, G., and Vanderkooi, J. M. (2003) Protein in sugar and glycerol/water as examined by IR spectroscopy and by the fluorescence and phosphorescence properties of tryptophan, *Biophys. J. 85*, 1980−1995.
26. Douzou, P. (1977) *Cryobiochemistry. An Introduction*, Academic Press, London.
27. Wright, W. W., Baez, C. J., and Vanderkooi, J. M. (2002) Mixed trehalose/sucrose glasses used for protein incorporation as studied by infrared and optical spectroscopy, *Anal. Biochem. 307*, 167−172.
28. Sievers, G. (1980) Structure of milk lactoperoxidase. A study using circular dichroism and difference absorption spectroscopy, *Biochim. Biophys. Acta 624*, 249−259.
29. Horie, T., Vanderkooi, J. M., and Paul, K. G. (1985) Study of the active site of horseradish peroxidase isoenzymes A and C by luminescence, *Biochemistry 24*, 7935−7941.
30. Hu, S., Treat, R. W., and Kincaid, J. R. (1993) Distinct heme active-site structure in lactoperoxidase revealed by resonance Raman spectroscopy, *Biochemistry 32*, 10125−10130.
31. Schonbaum, G. R., and Lo, S. (1972) Interaction of peroxidases with aromatic peracids and alkyl peroxides. Product analysis, *J. Biol. Chem. 247*, 3353−3360.
32. Fidy, J., Holtom, G. R., Paul, K. G., and Vanderkooi, J. M. (1991) Binding of naphthohydroxamic acid to horseradish peroxidase monitored by zinc mesoporphyrin fluorescence line narrowing, *J. Phys. Chem. 95*, 4364−4370.
33. Fidy, J., Paul, K. G., and Vanderkooi, J. M. (1989) Differences in the binding of aromatic substrates to horseradish peroxidase revealed by fluorescence line narrowing, *Biochemistry 28*, 7531−7541.
34. Schonbaum, G. R. (1973) New complexes of peroxidase with hydroxamic acids, hydrazides and amides, *J. Biol. Chem. 248*, 502−511.
35. Sievers, G., Peterson, J., Gadsby, P. M. A., and Thomson, A. J. (1984) The nitrosyl compound of ferrous lactoperoxidase, *Biochim. Biophys. Acta 785*, 7−13.
36. Dong, A., and Lam, T. (2005) Equilibrium titrations of acid-induced unfolding-refolding and salt-induced molten globule of cytochrome *c* by FT-IR spectroscopy, *Arch. Biochem. Biophys. 1436* (1), 154−160.
37. Manthey, J. A., Boldt, N. J., Bocian, D. F., and Chan, S. I. (1986) Resonance Raman studies of lactoperoxidase, *J. Biol. Chem. 261*, 6734−6741.
38. Goff, H. M., Gonzalez-Vergara, E., and Ales, D. C. (1985) High-resolution proton nuclear magnetic resonance spectroscopy of lactoperoxidase, *Biochem. Biophys. Res. Commun. 133*, 794−799.
39. Shiro, Y., and Morishima, I. (1986) Structural characterization of lactoperoxidase in the heme environment by proton NMR spectroscopy, *Biochemistry 25*, 5844−5849.
40. Kaposi, A. D., Fidy, J., Manas, E. S., Vanderkooi, J. M., and Wright, W. W. (1999) Horseradish peroxidase monitored by infrared spectroscopy: Effect of temperature, substrate and calcium, *Biochim. Biophys. Acta 1435*, 41−50.
41. Manas, E. S., Getahun, Z., Wright, W. W., DeGrado, W. F., and Vanderkooi, J. M. (2000) Infrared Spectra of Amide Groups in α-Helical Proteins: Evidence for Hydrogen Bonding between Helices and Water, *J. Am. Chem. Soc. 122*, 9883−9890.
42. Zelent, B., Nucci, N. V., and Vanderkooi, J. M. (2004) Liquid and ice water and glycerol/water glasses compared by infrared spectroscopy from 295 to 12 K, *J. Phys. Chem. A 108*, 11141−11150.
43. Cupane, A., Leone, M., Vitrano, E., and Cordone, L. (1995) Low-temperature optical absorption spectroscopy: An approach to the study of stereodynamic properties of hemeproteins, *Eur. Biophys. J. 23*, 385−398.
44. Edholm, O., Nordlander, P., Chen, W., Ohlsson, P.-I., Smith, M. L., and Paul, J. (2000) The effect of water on the Fe^{3+}/Fe^{2+} reduction potential of heme, *Biochem. Biophys. Res. Commun. 268*, 683−687.
45. Ikeda-Saito, M., Lee, H. C., Adachi, K., Eck, H. S., Prince, R. C., Booth, K. S., Caughey, W. S., and Kimura, S. (1989) Demonstration that spleen green hemeprotein is identical to granulocyte myeloperoxidase, *J. Biol. Chem. 264*, 4559−4563.
46. Hori, H., Fenna, R. E., Kimura, S., and Ikeda-Saito, M. (1994) Aromatic substrate molecules bind at the distal heme pocket of myeloperoxidase, *J. Biol. Chem. 269*, 8388−8392.
47. Blumberg, W. E., and Peisach, J. (1971) in *Bioinorganic Chemistry, Advances in Chemistry Series* (Eichorn, D., Ed.) pp 271−291.
48. De Gioia, L., Ghibaudi, E. M., Laurenti, E., Salmona, M., and Ferrari, R. P. (1996) A theoretical three-dimensional model for lactoperoxidase and eosinophil peroxidase, built on the scaffold of the myeloperoxidase X-ray structure, *J. Biol. Inorg. Chem. 1*, 476−485.
49. Tada, T., Watanabe, Y., Matsuoka, A., Ikeda-Saito, M., Imai, K., Ni-hei, Y., and Shikama, K. (1998) African elephant myoglobin with an unusual autooxidation behavior: Comparison with the H64Q mutant of sperm whale myoglobin, *Biochim. Biophys. Acta 1387*, 165−176.
50. Engler, N., Prusakov, V., Ostermann, A., and Parak, F. G. (2003) A water network within a protein: Temperature-dependent water ligation in H64V-metmyoglobin and relaxation to deoxymyoglobin, *Eur. Biophys. J. 31*, 595−607.
51. Edholm, O., Ohlsson, P. I., Smith, M. L., and Paul, J. (1998) The barrier for heme-protein separation estimated by non-equilibrium molecular dynamics simulations, *Chem. Phys. Lett. 291*, 501−508.

BI0513655